Development of arrays of position-sensitive microcalorimeters for Constellation-X

Stephen J. Smith[*,a,b] , Simon R. Bandler[a,c], Regis P. Brekosky[a,d], Ari -D. Brown[a,b], James A. Chervenak[a], Megan E. Eckart[a,b], Enectali Figueroa-Feliciano[e], Fred M. Finkbeiner[a,f], Richard L. Kelley[a], Caroline A. Kilbourne[a], F. Scott Porter[a], John E. Sadleir[a,g]
[a]NASA Goddard Space Flight Center, Greenbelt, MD 20771, USA;
[b]NASA Postdoctoral Program Resident Research Associate;
[c]CRESST and University of Maryland, College Park, MD 20742, USA;
[d]Northrop Grumman Corporation, Lanham, MD 20706, USA;
[e]Massachusetts Institute of Technology, Cambridge, MA 02139, USA
[f]Wyle Information Systems, McLean, VA 22102 USA;
[g]Department of Physics, University of Illinois Urbana-Champaign, Urbana, IL 61801, USA.

ABSTRACT

We are developing arrays of position-sensitive transition-edge sensor (PoST) X-ray detectors for future astronomy missions such as NASA's Constellation-X. The PoST consists of multiple absorbers thermally coupled to one or more transition-edge sensor (TES). Each absorber element has a different thermal coupling to the TES. This results in a distribution of different pulse shapes and enables position discrimination between the absorber elements. PoST's are motivated by the desire to achieve the largest possible focal plane area with the fewest number of readout channels and are ideally suited to increasing the Constellation-X focal plane area, without comprising on spatial sampling. Optimizing the performance of PoST's requires careful design of key parameters such as the thermal conductances between the absorbers, TES and the heat sink, as well as the absorber heat capacities. Our new generation of PoST's utilizes technology successfully developed on high resolution (~ 2.5 eV) single pixels arrays of Mo/Au TESs, also under development for Constellation-X. This includes noise mitigation features on the TES and low resistivity electroplated absorbers. We report on the first experimental results from new one-channel, four-pixel, PoST's or 'Hydras', consisting of composite Au/Bi absorbers. We have achieved full-width-at-half-maximum energy resolution of between 5-6 eV on all four Hydra pixels with an exponential decay time constant of 620 μs. Straightforward position discrimination by means of rise time is also demonstrated.

Keywords: transition-edge sensor, microcalorimeter, Constellation-X, imaging array, position-sensitive detector

1. INTRODUCTION

We are developing arrays of transition-edge sensors (TES's) for the X-ray Microcalorimeter Spectrometer (XMS) instrument on NASA's Constellation-X mission [1]. The Constellation-X reference configuration we consider here is based around a 10 m focal length with 5.5x5.5 arc minute field-of-view and 5 arc second position resolution. This is coupled with a full-width-half-maximum (FWHM) energy resolution of 2.5 eV (at an energy of 6 keV) over the center 2.75x2.75 arc minutes of the array at count rates of 1000's per pixel per second. The outer section of the array requires < 10 eV at more modest rates of a 10-100's counts per pixel per second. This configuration enables the study of bright, variable astrophysical point sources at high spectral resolution as well as extended sources. Figure 1 shows a schematic of the proposed focal plane layout.

[*] Corresponding Author. email: stephen.j.smith@nasa.gov; tel.:1-301-286-3719; fax: 1-301-286-1684.

Space Telescopes and Instrumentation 2008: Ultraviolet to Gamma Ray, edited by Martin J. L. Turner, Kathryn A. Flanagan, Proc. of SPIE Vol. 7011, 701126, (2008) · 0277-786X/08/$18 · doi: 10.1117/12.790100

2. POSITION-SENSITIVE DETECTORS

In order to meet the stringent resolution and count-rate requirements of the central field-of-view elements, we are developing a 32x32 single pixel TES array (250 μm pixel pitch) [2]. The high density of electrical wiring and increased heat loads from bias and read-out circuitry make a single pixel array a less favorable option for providing the outer focal-plane elements (3072) of the XMS, and warrant an alternative approach. Consequently, we are pursuing position-sensitive TES's (PoST's) [3,4]. PoST's consist of multiple absorber elements each with a different thermal coupling to one or more TES. This differential thermal diffusion to the sensor results in a characteristic pulses shape for each absorber element and enables position discrimination. PoST's are well suited to increasing the field of view for missions such as Constellation-X without significantly increasing the number of required read-out channels.

Compared to their single pixel equivalents, the PoST design will in general suffer from a degraded energy resolution and count-rate capability. The energy resolution of a microcalorimeter scales with the square root of the total heat capacity C, so an N absorber PoST with a single read-out sensor will suffer a $N^{1/2}$ degradation in energy resolution. Furthermore, a loss in maximum count-rate capability per spatial sampling element of ~ N^2 will result due to an N times slower thermal decay (decay time varies as $1/C$) coupled with the N times larger area

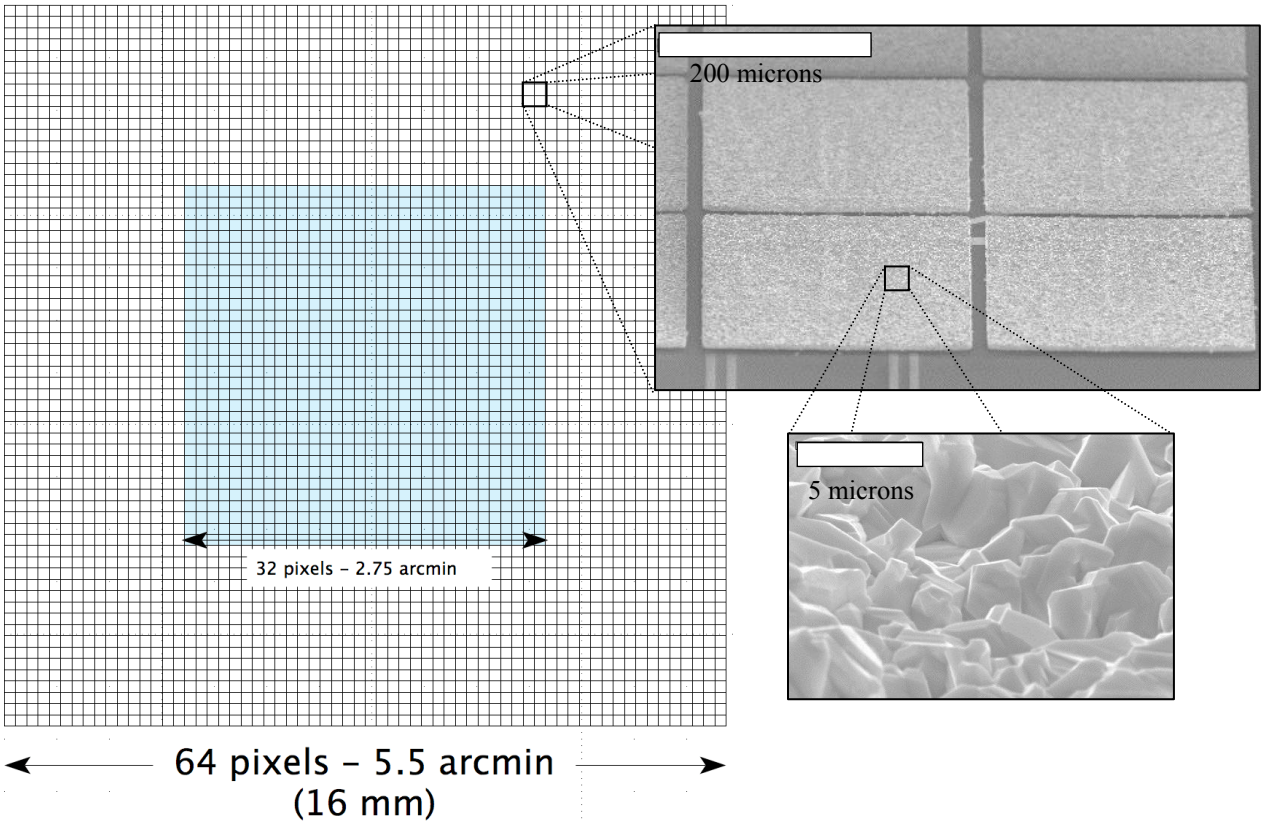

Fig. 1. Schematic diagram of a large format imaging array such as that proposed for Constellation-X. The first inset shows a SEM image of a four pixel PoST which is read-out using a single TES beneath one of the absorbers. The second inset shows a magnification of the composite Au/Bi absorber surface showing the individual grains of bismuth, which are typically several microns in size. When an X-ray photon is absorbed in a grain it thermalizes vertically before equilibrating with the rest of the absorber through the Au layer.

The conventional approach to designing a PoST has been to readout a one-dimensional, continuous or segmented, absorber with TES's at both ends [3,5-6]. In this configuration, the sum of the TES signals gives energy information and the difference between the signals yields position information. Using a segmented absorber simplifies the position

determination; since instead of having a continuum of pulse shapes we have a discrete population corresponding to each absorber segment, which we can refer to as a pixel. The energy of the photon can then be calculated using a single stored digital optimal filter referenced for each pixel. Although using more than one sensor to read-out a PoST is advantageous from the point of view of position discrimination, it is not actually necessary. Position information is encoded in the pre-equilibration pulse shape, thus it is possible to make a PoST by connecting several absorbers to a single TES via varied thermal links. This is attractive for several reasons. Firstly, two-channel PoST's perform best when the TES's have exactly the same transition temperatures. A need to establish even a small temperature gradient across the high-conductivity absorber will require a significant difference in the bias power applied to each TES. Secondly, the electrical grounds of the two TES's are connected via the absorber. For common-bias schemes to work, this will require a very small common shunt resistor. Furthermore, for the same number of pixels per TES, the heat capacity and hence the energy resolution will be better in a 1-TES PoST. Therefore, in addition to the 2-channel PoST's, we are developing single-channel PoST's or 'Hydras' [4].

Figure 2 shows average pulse shapes from a typical Hydra design as described in Section 3, also shown is a simple thermal model of the Hydra concept showing four absorbers with different thermal couplings to a single TES. By controlling the thermal conductance of the internal links G_L, it is possible to optimize the Hydra design for position discrimination or energy resolution. In the limit of high internal link conductance relative to the bath conductance $G_L/G_b \rightarrow \infty$, the Hydra will act as a single pixel with optimum energy resolution but no position discrimination. By slowing the internal links to different values we can introduce position discrimination between the different pixels. However, in doing so we introduce internal thermal fluctuation noise between the absorbers and the TES, which degrades the energy resolution. Thus there is an intrinsic trade-off between the energy resolution and position sensitivity. The ability to discriminate between pulses varies inversely with photon energy, thus the Hydra must be designed to give position sensitivity at the lowest energies of interest. Using the models and signal processing algorithms described in refs [4,7-8] we can optimize the Hydra heat capacities and thermal conductances to give equal position discrimination between pixels, coupled with optimum energy resolution.

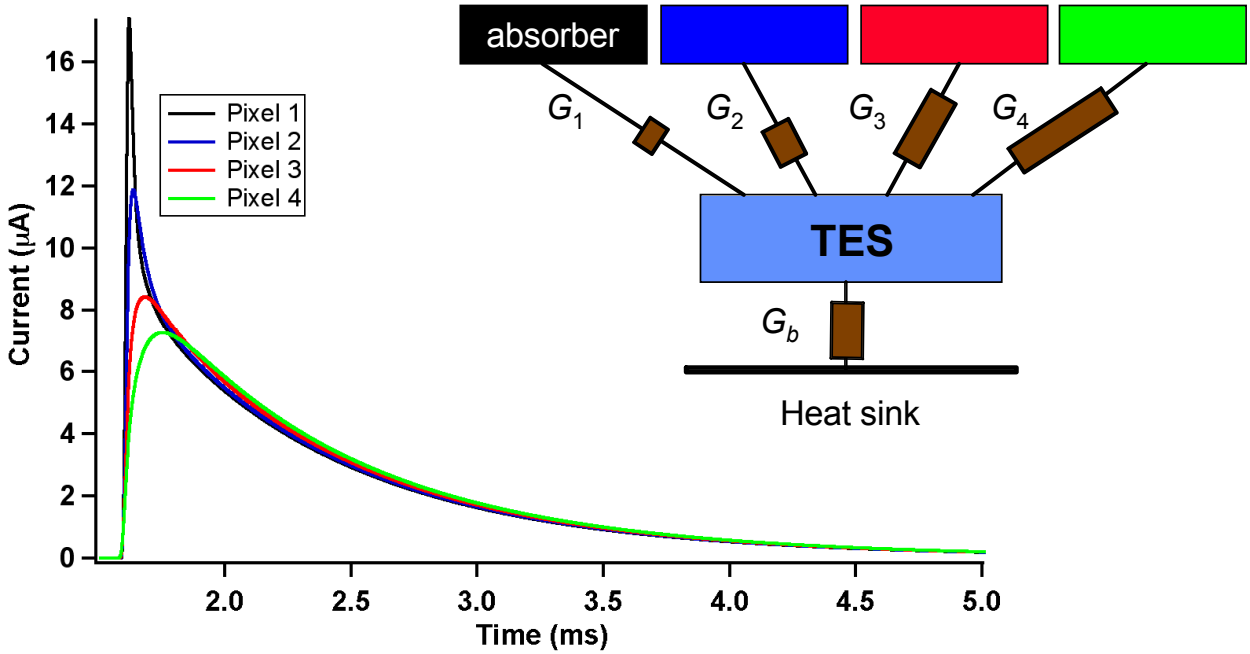

Fig. 2. Experimentally measured average pulse shapes for typical Hydra design described in Section 3. After the initial position-dependent equilibration signal the pulses decay with the same exponential rate. The inset shows a simple thermal model of the Hydra concept including four absorbers with different thermal couplings to a TES, which is in turn weakly thermally coupled to a heat sink.

3. DETECTOR DESIGN AND FABRICATION

The Hydra design is based around our successful development of single pixel Mo (45 nm)/Au (200 nm) bilayer TES's with electroplated, vacuum-gap, Au and composite Au/Bi absorbers [6,7]. Using composite absorbers allows us to tune the heat capacity of the device for optimum energy resolution whilst maintaining a high quantum efficiency (QE). The TES's are deposited onto low stress silicon-nitride membranes of thickness typically 1-2 μm. Atop the TES we deposit normal metal (Au) features such as banks along the side of the TES, which improve the uniformity of the superconducting-to-normal transition [10], and interdigitated stripes, which reduce the excess noise in our TES's [11]. The electroplated bismuth has grain sizes of typically several microns and has an order of magnitude lower electrical resistivity than our evaporated bismuth [12]. These high purity electroplated absorbers are designed for rapid thermal diffusion of the X-ray photon energy to the TES. The absorbers are connected to the TES via 'T' shaped stems, which are designed to minimize additional normal metal contact area with the TES that has the potential to change its performance. This technology has enabled us to produce uniform 8x8 arrays of single pixel TES's with FWHM energy resolution of ~ 2.5 eV and decay times ~ 500 μs [13].

The first Hydra pixel is identical to our baseline pixel design, consisting of an electroplated vacuum-gap absorber strongly thermally coupled directly to the TES via a 'T'-stem. Three additional electroplated absorbers are supported directly on the silicon-nitride via identical 'T'-stems. The silicon-nitride membranes are 418x418 μm^2. For the first fabrication runs we choose 1 μm Au with 4 μm Bi atop. The bismuth layer provides a significant fraction of the stopping power whilst the Au provides rapid thermal diffusion. The total quantum efficiency of the absorber is ~ 95 % at 6 keV. The lateral dimensions of the absorber are 236 μm. These pixels are thermally coupled to the TES pixel via Ti (20 nm)/Au (200 nm) metal links which are deposited by electron-beam evaporation and have an electrical resistivity of 0.37 μΩ-cm at 4.2 K. We vary the length (64-802 μm) and width (7.7-18.3 μm) of the links to tune the thermal conductance to the necessary value. The heat capacity of the links are designed to contribute no more than ~ 1 % of the total heat capacity of the Hydra.

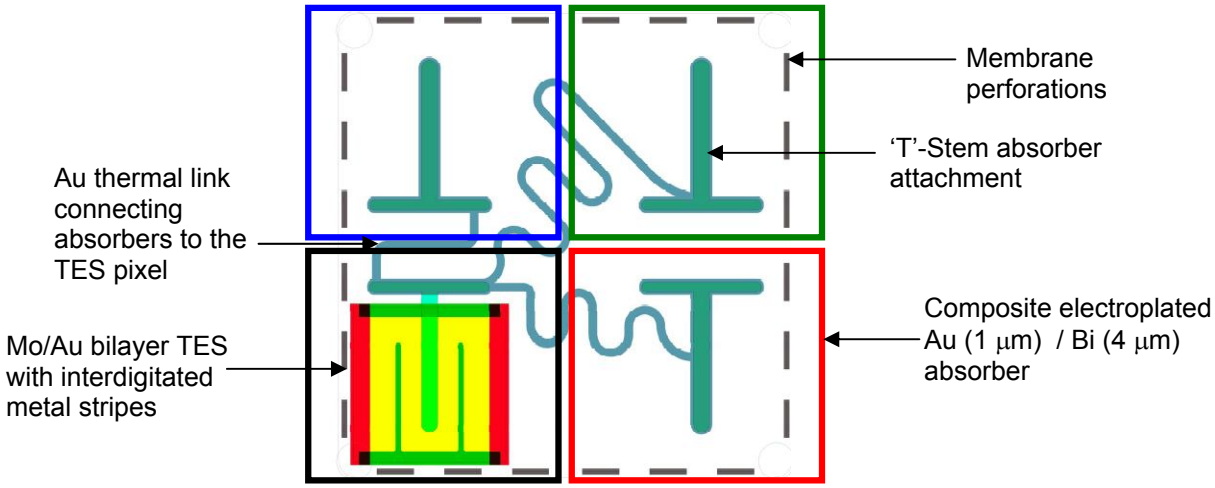

Fig. 3. Schematic diagram of the Hydra concept, which shows four absorber outlines with 'T'-stems thermally coupled to the TES via thin Au links.

The thermal conductance between the TES and the heat sink is controlled by the silicon-nitride membrane. For a fixed membrane thickness *d*, this conductance has been shown to scale with only the perimeter of the TES in contact with the membrane [14]. The Hydra design has a significantly more complex geometry than our single pixel TES's and the phonon emitting perimeter is likely to be several times larger. Although a larger thermal conductance to the bath is preferential for achieving high speed, the larger operating current can result in non-ideal effects such as an increase in excess noise. For our single pixel devices, perforations around perimeter of the TES are shown to proportionally reduce the phonon emitting area and hence the conductance to the bath [14]. To investigate the performance of these devices with different thermal conductances to the heat sink we have added different levels of perforations around the edge of

the Hydra membrane. Four different chip types were fabricated with different levels of membrane perforations, 0 %, 50 % and 75 %. On each chip we fabricated 24 Hydra's with three different sets of internal links. In total, there were five different sets of links to cover all four membrane perforation levels.

4. RESULTS AND ANALYSIS

Different chips from two different wafers were tested on several experimental runs in an adiabatic demagnetization refrigerator (ADR) with an operational base temperature of ~ 50 mK. The devices were read-out using SQUID's, provide by Physikalisch-Technische Bundesanstalt (PTB, Berlin), with low total circuit inductance of typically 10-20 nH [15]. This allowed us to characterize the intrinsic pulse shapes without significant attenuation from the readout electronics. Devices were illuminated using an ^{55}Fe X-ray source (~ 100 μCi) which provided a flux of Mn-Kα and Mn-Kβ X-rays of energy 5898 and 6490 eV respectively. A small copper collimator reduced the number of background frame hits to a minimal level. The measured count-rate per Hydra was of the order a few per second. Data acquisitions were typically over ~ 6 hr periods over which time several 10,000's of pulses were logged using a 14-bit analogue-to-digital (ADC) converter.

On the first fabricated wafer we measured a transition temperature of ~ 86 mK, uniform across many devices. The thermal conductance to the bath G_b ranged between 0.5 nW/K and 1.4 nW/K (at 100 mK) across numerous devices with different membrane perforations. However these data were not correlated with the level of perforation and it was subsequently found from scanning electron microscope (SEM) images that the absorbers had drooped at the edges causing a direct thermal short to the silicon frame. This was found to be a common feature of all devices though the degree of the thermal shorts varied significantly. This can result in non-idea effects such as athermal phonon loss directly to the frame [16] and non-uniform equilibration of the absorbers. In addition, the internal links were designed to give optimal energy resolution for a bath conductance of between ~ 100-500 pW/K (at 100 mK), thus many of these devices were far from optimized. On a second fabrication run we optimized processing steps and fixed this problem, however the transition temperature was slightly higher at 106 mK. The device heat capacity was measured at ~ 1.9 pJ/K (at 100 mK). Figure 1 includes SEM images of the Hydra absorbers from this second wafer. Table 1 shows a summary of the internal and external thermal conductances for several devices. Hydra 1 is from the first wafer and Hydras 2-4 from the second wafer. Also shown is the measured energy resolution from Mn-Kα X-ray testing and the baseline resolution. Despite the drooping absorbers, we were still able to achieve impressive FWHM energy resolution of around 5-6 eV (close to the measured baseline resolution) on this one particular device from the first wafer. For this device the thermal conductance was ~ 40 % in excess of that expected without any thermal short to the frame. The thermal decay time was 620 μs. Figure 4 shows an Mn-Kα spectrum for Hydra 1 pixel 2 with an energy resolution of 5.05±0.14 eV. Hydras 2-4 from wafer 2 have approximately the same thermal conductance to the bath but different internal link strengths (fast, medium and slow respectively). The energy resolution of a microcalorimeter scales approximately as $T^{3/2}$, thus the higher transition temperature of the second wafer degraded the resolution from ~ 5 eV on wafer 1 to ~ 7 eV.

Table 1. Internal ($G_{2\text{-}4}$) and external (G_b) thermal conductances for 4 different Hydra devices (referenced at 100 mK). Also shown is the optimally filtered FWHM energy resolution for the 4 Hydra pixels at 5.9 keV ($\Delta E_{1\text{-}4}$) and the optimally filtered baseline resolution ($\Delta E_{B1\text{-}4}$). The heat capacity of the devices was estimated to be ~ 1.9 pJ/K (at 100 mK) and the transition temperatures were 86 and 106 mK for wafers 1 and 2 respectively. All these devices were fabricated on 50% perforated membranes.

Hydra	G_b (nW/K)	G_2 (nW/K)	G_3 (nW/K)	G_4 (nW/K)	$\Delta E_{1\text{-}4}$ (eV)	$\Delta E_{B1\text{-}4}$ (eV)	τ (ms)
1	0.58	29.7	12.1	6.6	5.85, 5.05, 6.04, 5.63	3.75, 4.46, 5.40, 5.69	0.62
2	0.45	29.7	12.1	6.6	7.66, 6.70, 7.25, 7.57	5.10, 5.84, 6.68, 7.26	0.83
3	0.39	15	6.1	3.3	7.69, 6.65, 7.56, 8.82	5.33, 6.89, 8.07, 8.94	0.81
4	0.43	6.1	2.5	1.35	7.10, 7.55, 9.30, 10.00	4.48, 7.16, 8.70, 9.98	0.99

For all Hydras in Table 1, the Mn-Kα energy resolution for the best coupled pixel to the TES had quadratic broadening above the listed baseline resolutions. For Hydra 1 this broadening was 6.6 eV and for Hydras 2-4 this was 13.5, 10.5 and 8.5 eV respectively, apparently decreasing with slower internal link conductances. By applying a low pass filter of between 5-7.5 kHz to the digital optimal filter, effectively suppressing high frequency components in the signal band, we were able to improve the resolutions to a comparable level to the other pixels (as is listed in Table 1). In doing so, we reduce the useable bandwidth and degrade baseline resolution. This behavior shows there are high frequency fluctuations in the signal band on a pulse-by-pulse basis, and is strongly indicative of position dependence within the absorber [17]. Due to contamination of the Au electroplating solution on wafer 2, the low temperature (4.2 K) electrical resistivity of the absorber material was degraded by ~ 2.5 times that of the first wafer. This is a likely reason why the broadening terms were significantly worse for the second wafer, since the electrical resistivity is inversely proportional to the thermal diffusivity. Absorber pixels 2-4 do not show any broadening above the baseline resolution because they are thermally decoupled form TES. Thus any high frequency position dependent signal components are naturally suppressed through the thermal links. The degree of position dependence will in general depend upon the ratio of the conductance out of the absorber to the conductance within the absorber. If energy leaves the absorber before the absorber has fully equilibrated then position dependence can occur. The pre-equilibration signal of the Hydra is intrinsically sensitive to position dependent broadening because the conductance out the first pixel to the other three is typically high (around 50 nW/K for Hydra 1 for example). In our single pixel TES the only energy loss from the absorber is via the TES, which typically has an electro-thermal conductance of around 1-2 nW/K. This evidence suggests that a significant increase in the absorber diffusivity is required to eliminate position dependence in these absorber pixels. On future fabrication runs we will investigate optimizing the ratio of the Au/Bi thickness for improved absorber diffusivity.

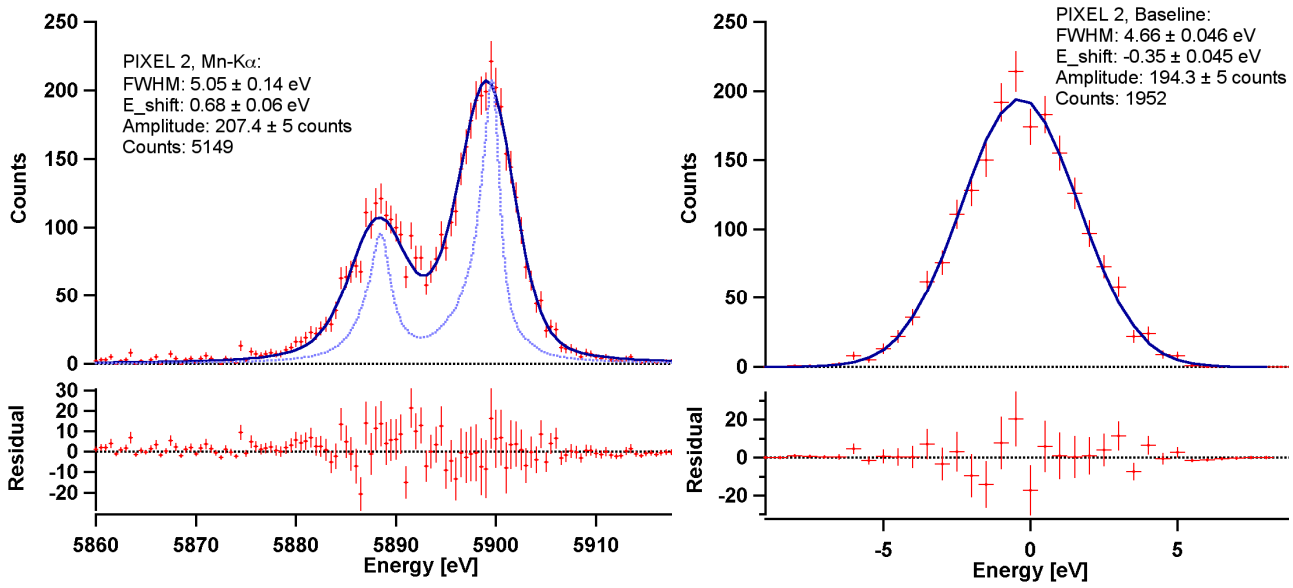

Fig 4. Left: A spectrum of Mn-Kα X-rays from an ^{55}Fe source for Hyrda 1 pixel 2 (as listed in Table1) with Bi/Au absorber. The instrumental function is consistent with a Gaussian response with a resolution of 5.05±0.14 eV FWHM. The dashed line shows the intrinsic line shape from Hölzer et al. [18], with correction and extension provided by Hölzer via private communication. Right: Gaussian fit to the baseline noise.

For all these devices position discrimination at 6 keV was easily demonstrated from pulse-height versus rise-time (20-80%) analysis. Figure 5 shows raw pulse-height/rise-time data from typical data set for Hydra 2. The Mn-Kα distributions are marked on the plot and the pixels are clearly well separated. Figure 5 also shows the average pulse height-rise time of many pulses for Hydras 2-4 with the fast, medium and slow thermal links. The measured rise times show very good agreement with theoretically modeled values. Slowing the internal links increases the separation between the pulses but degrades the resolution because of the increased thermal fluctuation noise. Constellation-X requires position sensitivity down to energies as low as 300 eV, thus in future runs will we utilize low energy X-ray

sources to investigate position sensitivity at energies of 1.5 keV and below. Although clearly adequate at the higher energies, rise-time discrimination is non-optimal and may not be an accurate technique in the low energy range. We are investigating digital signal processing algorithms based around the optimal filter, which allow theoretically optimized determination of event position [4,7] down to much lower energies. We will be implementing these algorithms on real data in the near future. Such algorithms will allow us to further tune the thermal conductances for optimum energy and position sensitivity.

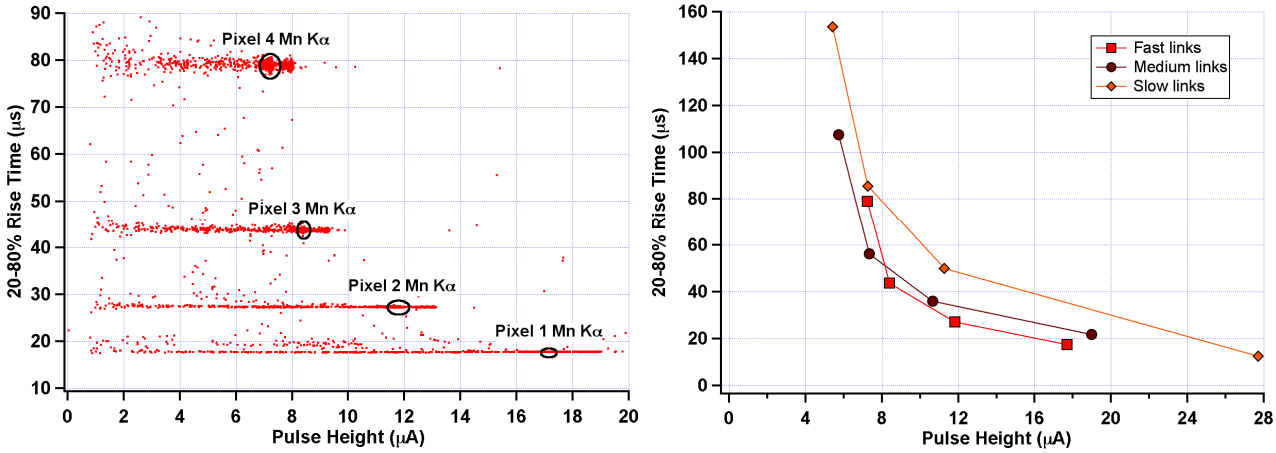

Fig 5. Left: Raw rise time vs. pulse height for Hydra 2 (see Table 1) for Mn-Kα and Mn-Kβ X-rays. The low energy continuum is due to electron loss events and accounts for ~ 3 % the total events. Right: Average rise time vs. pulse height for Hydra 2-4, which have fast, medium and slow internal links respectively, and approximately the same thermal conductance to the bath. Figure 2 shows the average of the pulses shapes corresponding to Hydra 2 with the fastest link configuration.

5. CONCLUSION

We have demonstrated the first experimental results for four-pixel position-sensitive Hydras. These first generation devices demonstrate proof of concept and already meet the initial target specifications for energy resolution and decay time for Constellation-X. The best results have demonstrated a FWHM energy resolution of between 5.1 and 6.0 eV across all four pixels with a pulse decay time of ~ 620 μs. Straightforward position discrimination, using pulse rise time, has been demonstrated at 6 keV. A > 6 eV broadening in the energy resolution of the most strongly coupled absorber to the TES, has been attributed to position dependence within the absorber. By bandwidth limiting the optimal filter we were able to reduce this broadening to a level which gives comparable resolution to the other pixels. Further studies are required in order to optimize the relative thicknesses of the Au/Bi in order to improve diffusivity whilst maintaining low heat capacity for optimum energy resolution. In addition to these 4-pixel designs, we intend to investigate 6 and 9-pixel Hydras. Such devices would further decrease the number of read-out channels for the Constellation-X extended field-of-view, whilst maintaining a theoretical energy resolution of 10 eV or less.

ACKNOWLEDGMENTS

This research was in part supported by appointments (A.–D. Brown, M.E. Eckart, and S.J. Smith) to the NASA Postdoctoral Program at Goddard Space Flight Center, administered by Oak Ridge Associated Universities through a contract with NASA. We would like to thank Jörn Beyer (PTB-Berlin) for providing state-of-the art SQUID's that have been used in this work.

REFERENCES

[1] Hornschemeier A. E., White N. E., and Tananbaum H., "The frontier in x-ray spectroscopy: NASA's Constellation-X mission" AIP Conf. Proc. 774, 383 (2005).

[2] Iyomoto N., Bandler S. R., Brekosky R. P., Brown A. -D., Chervenak J. A., Finkbeiner F. M., Kelley R. L., Kilbourne C. A., Porter F. S., Sadleir J. E., Smith S. J., and Figueroa-Feliciano E., "Close-packed arrays of transition-edge x-ray microcalorimeters with high spectral resolution at 5.9 keV," Appl. Phys. Lett. 92, 013508 (2008).

[3] Iyomoto N., Bandler S. R., Brekosky R. P., Chervenak J. A., Figueroa-Feliciano E., Finkbeiner F. M., Kelley R. L., Kilbourne C. A., Lindeman M. A., Murphy K., Porter F. S., T. Saab, Sadleir J. E. and Talley D. J., "Position-sensitive transition-edge sensors", Nucl. Instr. and Meth. A 559, 491-493 (2006).

[4] Smith S. J., Bandler S. R., Brown A. -D., Chervenak J. A., Figueroa-Feliciano E., Finkbeiner F. M., Iyomoto N., Kelley R. L., Kilbourne C. A. and Porter F. S., "Optimizing arrays of position sensitive TES's", Journal of Low Temperature Physics 152, 1009-1014 (2008).

[5] Smith S. J., Whitford C. H., Fraser G. W. and Goldie D. J., "Characterisation and modelling of transition edge sensor distributed read-out imaging devices", Nucl. Instr. and Meth. A 559(2), 500-502 (2006).

[6] Stern R. A., Rausch A., Deiker S., Martínez-Galarce D., Shing L., Irwin K. D., Ullom J. N., O'Neil G., Hilton G. and Vale L., "X-ray Microcalorimeter Research for Solar Physics at LMSAL and NIST: An Update", Journal of Low Temperature Physics 152, 721-726 (2008).

[7] Smith S. J., Whitford C. H. and Fraser G. W., "Optimised filtering for improved energy and position resolution in position-sensitive TES based X-ray detectors", Nucl. Instr. and Meth. A 556, 237 (2006).

[8] Figueroa-Feliciano E., "Complex microcalorimeter models and their application to position-sensitive detectors", J. Appl. Phys. 99, 114513 (2006).

[9] Bandler S. R., Brown A. -D., Chervenak J. A., Figueroa-Feliciano E., Finkbeiner F., Iyomoto N., Kelley R. L., Kilbourne C. A., Porter F. S. and Smith S. J., "Performance of TES X-ray Microcalorimeters with a Novel Absorber Design", Journal of Low Temperature Physics 151, 400 (2008).

[10] Hilton G. C., Martinis J. M., Irwin K. D., Bergren N. F., Wollman D. A., Huber M. E., Deiker S. and Nam S. W., "Microfabricated Transition-Edge X-ray Detectors", IEEE Transactions on Applied Superconductivity 11, 739 (2001).

[11] Ullom J. N., Doriese W. B., Hilton G. C., Beall J. A., Deiker S., Duncan W. D., Ferreira L., Irwin K. D., Reintsema C. D. and Vale L. R., "Characterization and reduction of unexplained noise in superconducting transition-edge sensors", Appl. Phys. Lett. 84, 4206-4208 (2004).

[12] Brown A. -D., Bandler S. R., Chervenak J. A., Figueroa-Feliciano E., Finkbeiner F. M., Iyomoto N., Kelley R.L., Kilbourne C. A., Porter F. S., Saab T., Sadleir J. and Smith S. J., "Absorber Materials for Transition-Edge Sensor X-ray Microcalorimeters", Journal of Low Temperature Physics 151, 413-417 (2008).

[13] Kilbourne C. A., Bandler S. R., Brown A. -D., Chervenak J. A., Figueroa-Feliciano E., Finkbeiner F. M., Iyomoto N., Kelley R. L., Porter F. S. and Smith S. J., "Uniform high spectral resolution demonstrated in arrays of TES x-ray microcalorimeters", Proc. SPIE 6686, 668606 (2007).

[14] Stahle C. K., Lindeman M. A., Figueroa-Feliciano E., Li M. J., Tralshawala N., Finkbeiner F. M., Brekosky R. P. and Chervenak J. A., "Arraying compact pixels of transition-edge microcalorimeters for imaging x-ray spectroscopy", Proceedings of the 9th International Workshop on Low Temperature Detectors, AIP Conference Proceedings 605, 223 (2001).

[15] Drung D., Assmann C., Beyer J., Kirste A., Peters M., Ruede F. and Schurig T., "Highly Sensitive and Easy-to-Use SQUID Sensors", IEEE Transactions on Applied Superconductivity 17(2), 699-704 (2008).

[16] Kilbourne C. A., Bandler S. R., Brown A. -D., Chervenak J.A., Figueroa-Feliciano E., Finkbeiner F., Iyomoto N., Kelley R. L., Porter F. S. and Smith S. J., "Various Optimizations of TES Arrays for X-ray Astrophysics", Journal of Low Temperature Physics 151, 223 (2008).

[17] Saab T., Figueroa-Feliciano E., Iyomoto N., Bandler S. R., Chervenak J. A., Kelley R. L., Kilbourne C. A., Porter F. S. and Sadleir J. E., "Determining the thermal diffusivity in microcalorimeter absorbers and its effect on detector response", J. Appl. Phys. 102(10), 104502–104502-7 (2007).

[18] Hölzer G., Fritsch M., Deutsch M., Härtwig J., and Förster E., "$K_{1,2}$ and $K_{1,3}$ x-ray emission lines of then 3d transition metals," Phys. Rev. A 56, 4554–4568 (1997).